MINERALOGY OF THE SAHARA 97037 METEORITE: INSIGHTS FROM PETROGRAPHY, EPMA, AND RAMAN SPECTROSCOPY Faruq Anjorin[1], Steven J. Jaret[1,2,3], Rondi Davies[4], and Marina Gemma[2], [1]Department of Physical Sciences, Kingsborough Community College, Brooklyn, NY [2]Department of Earth and Planetary Sciences, American Museum of Natural History, New York, NY [3]CUNY Graduate Center, New York, NY, [4]Queensborough Community College, Queens, NY. Faruq.anjorin52@students.kbcc.cuny.edu

Introduction: Type 7 ordinary chondrites are rare meteorites that represent the highest degree of thermal metamorphism experienced by chondritic material [1,2]. At this metamorphic grade, primary chondrule textures are largely erased, mineral compositions fully equilibrated, and chemical and textural features record intense parent-body heating and recrystallization. As a result, type 7 chondrites provide important constraints on the thermal structure and internal evolution of ordinary chondrite parent bodies, yet they remain underrepresented in detailed spatially resolved studies.

Sahara 97037 is classified as an LL7 ordinary chondrite, belonging to the low-iron, low-metal group and representing one of the most thermally processed members of the LL series. Although its classification and general metamorphic state have been documented [3], Sahara 97037 has not been extensively studied using coordinated petrographic, geochemical, and spectroscopic techniques. In particular, spatially extensive chemical mapping and mineral identification across the sample remain limited, leaving key aspects of its internal heterogeneity and metamorphic history poorly constrained.

Methods: Sahara 97037 was investigated using a combination of optical microscopy, electron probe micro-analysis (EPMA), and Raman spectroscopy. Optical microscopy was conducted using an Olympus BH2 petrographic microscope. Backscatter imaging was conducted using a Hitachi S4700 field emission scanning electron microscope. EMPA analyses were conducted at the American Museum of Natural History using a 5-spectrometer Cameca SX5-Tactis. Wavelength dispersive spectroscopy (WDS) was used for both quantitative point analyses and elemental mapping. Point analyses used an accelerating voltage of 40 nA and spot size of 1 µm. Standardization was conducted on natural standards from the AMNH collection.

X-ray elemental mapping was conducted using a series of 3 passes each containing 5 elemental maps. Beam current was 40 nA with dwell time of 15 ms and step size of 6 µm. Full section maps are a mosaic of 15 EPMA maps. Raman analyses were performed using a WiTec Alpha300R confocal Raman microscope with a 532 nm laser operated at ~20 mW. Mapping used a 0.7 sec integration time, and a spectral grating of 300 grooves per millimeter. The spatial resolution for Raman mapping is 751 nm.

Results: Optically, the most striking feature in Sahara 97037 is a large, 2.9 mm, dark vein that is nearly opaque in transmitted light (Fig. 1). This vein exhibits a sharp boundary with the host olivine-dominated matrix.

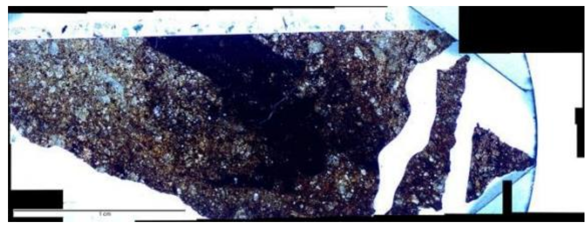

Figure 1: Plane-polarized light image of Sahara 97037.

High resolution SEM imaging shows the vein consists of fine grained (10-25 µm) euhedral olivine and pyroxene grains showing melt textures (Fig. 2). Pyroxene compositions are enstatite (En_{97}). The vein contains two compositions of olivine: Fo_{95} and Fo_{65}. In contrast, olivine and pyroxene grains adjacent to the vein are large (50-100 µm) and have granoblastic textures.

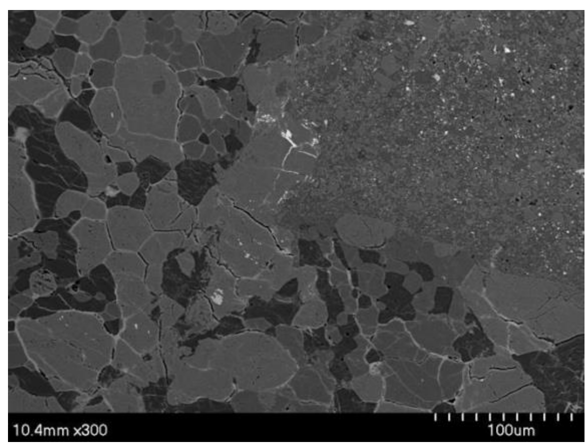

Figure 2: BSE image of the contact between the vein and the host meteorite.

Single-element X-ray maps reveal pronounced spatial heterogeneity across the sample (Fig. 3). The vein is enriched in Fe and Cr, but depleted Si relative to the host. The Mg X-ray map (Fig. 4) shows 3 compositionally distinct regions, identified based on Mg intensity. The vein itself is slightly enriched in Mg relative to the host, but region of granoblastic olivine and pyroxene immediately adjacent to the vein is highly enriched in Mg relative to both the host and the vein itself.

Raman spectroscopy of phases within the vein is complex (Fig. 5). We identified 4 phases. Phase 1 is olivine, with dominant peaks at 845 Δcm^{-1} and 820 Δcm^{-1}. These olivine grains exhibit another small peak at 912 Δcm^{-1}.

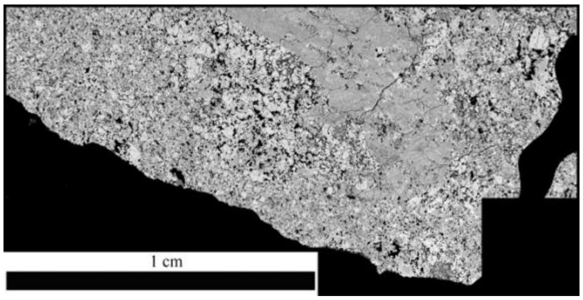

Figure 4: Single-element Mg X-ray map of Sahara 97037 showing spatial variations in Mg concentration across the sample. Bright regions indicate higher Mg intensity, while darker regions indicate lower Mg intensity. The prominent dark vein crosscutting the host lithology has a measured thickness of ~2.9 mm. Scale bar = 1 cm.

Phase 2 is pyroxene, with dominant peaks at 1006 Δcm^{-1} and a doublet near 687 Δcm^{-1}. This phase is most likely clinoenstatite, denoted by the doublet, although the primary peak is shifted to slightly lower wavenumbers than other meteoritic clinoenstatite. A similar Raman spectrum – including both the doublet and the peak at 1006 Δcm^{-1} was reported in shocked "vesicular pyroxene" from the Kamargaon L6 chondrite [4].

Phase 3 exhibits a broad peak near 678 Δcm^{-1} with lower intensity peaks at 216 Δcm^{-1} and 278 Δcm^{-1}. This phase is distinct from pyroxene as it lacks a strong peak at 1000 Δcm^{-1}. The best match for this spectrum is chromite, which is consistent with the Cr enrichment in the vein, and 15-20 µm chromite grains were observed under the SEM.

. Phase 4 is similar to phase 2, but exhibits a less intense characteristic pyroxene peak at 1000 Δcm^{-1}. This likely reflects the fine grained nature of pyroxenes within the matrix.

Discussion: We interpret the large vein as a shock-melt vein. Textures within the vein (Fig. 2) are consistent with melt textures seen in other ordinary chondrites. The presence of olivine and clinoenstatite suggest crystallization at elevated pressures, consistent with shock veins. Interestingly, we have not yet observed other high-pressure polymorphs such as wadsleyite or ringwoodite. Ongoing work will continue structural analysis of this vein margin where the coarse granoblastic texture adjacent to the vein is interpreted as due to contact metamorphism associated with the shock-melt vein.

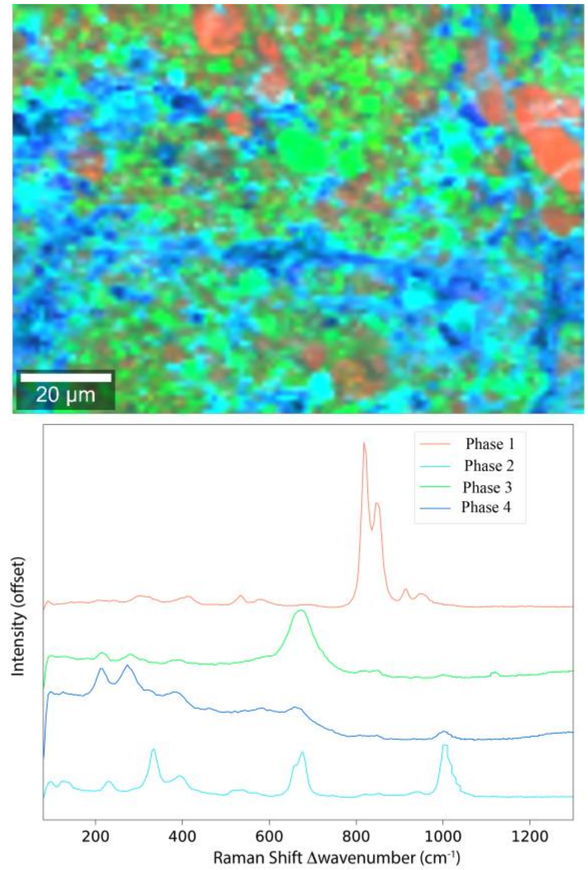

Figure 5. Raman image (top) and spectra (bottom) of mineral phases within the large vein. Phase 1 is olivine, phase 2 is pyroxene, phase 3 is chromite, phase 4 is pyroxene.

Acknowledgements: We thank Denton Ebel and the Museum of Natural History for curation of the sample. We thank Celine Martin for providing access to electron probe micro-analysis (EPMA) and Raman spectroscopy. This work was supported by the CUNY Research Scholars Program (CRSP).

References: [1] Huss G. R., Rubin A. E., and Grossman J. N. (2006). In Meteorites and the Early Solar System II (Lauretta D. S. and McSween H. Y., eds.), pp. 567–586, Univ. of Arizona. [2] Rubin A. E. (2010) GCA 74, 4807–4828. [3] Grossman J. N. et al. (1998) Meteoritical Bulletin, No. 82, 293–322. [4] Tiwari et al., 2022. JGR Planets. 127, e2022JE007420